Anion-Induced Urea Deprotonation

Massimo Boiocchi,[b] Laura Del Boca,[a] David Esteban-Gómez,[a] Luigi Fabbrizzi,*[a] Maurizio Licchelli,[a] and Enrico Monzani[a]

Abstract: The urea-based receptor **1** (1-(7-nitrobenzo[1,2,5]oxadiazol-4-yl)-3-(4-nitrophenyl)urea, L–H), interacts with X^- ions in MeCN, according to two consecutive steps: 1) formation of a hydrogen-bond complex $[L–H\cdots X]^-$; 2) deprotonation of L–H to give L^- and $[HX_2]^-$, as shown by spectrophotometric and ^{1}H NMR titration experiments. Step 2) takes place with more basic anions (fluoride, carboxylates, dihydrogenphosphate), while less basic anions (Cl^-, NO_2^-, NO_3^-) do not induce proton transfer. On crystallisation from a solution containing L–H and excess Bu_4NF, the tetrabutylammonium salt of the deprotonated urea derivative ($Bu_4N[L]$) was isolated and its crystal and molecular structure determined.

Keywords: acid–base reactions · anions · hydrogen bonds · supramolecular chemistry · urea

Introduction

There exists a large interest on the development of artificial neutral receptors for anions.[1–3] Such molecules should be able to behave as hydrogen-bond donors towards the envisaged anion, giving rise to a complex that is stable in solution. One of the most frequently employed fragments is urea. In fact, urea can donate two hydrogen bonds in a parallel fashion, and so it is complementary to Y-shaped oxoanions such as carboxylates. One of the first examples of anion complexation by urea-based receptors was reported by Wilcox, who characterised the receptor–analyte interaction through ^{1}H NMR experiments and determined the association constant of the complex by spectrophotometric titrations.[4] A variety of receptors containing one or more urea subunits have been designed and tested for anion recognition and sensing over the past years.[5–12] A major element of selectivity is given by the energy of the receptor–anion interaction: in fact, the strongest hydrogen-bond interactions are established with anions that contain the most electronegative atoms, for example, F (fluoride) and O (carboxylates, inorganic oxoanions), and that display the most pronounced basic tendencies in the chosen solvent. On the other hand, in most cases electron-withdrawing substituents have been appended to the urea framework in order to polarise the N–H bonds and to increase its hydrogen-bond donor tendencies. Therefore, the strongest interactions are expected to occur between highly basic anions and highly acidic urea fragments; this opens the way to the potential occurrence of an acid–base process, with neat proton release from urea to the anion. Very interestingly, the hydrogen-bonding interaction has been recently defined as an "incipient" and "frozen" proton-transfer process.[13] On this basis, we were interested to verify whether urea, in presence of suitable anions, may undergo deprotonation in solution.

In this context, we studied the interaction of the urea derivative **1** (1-(7-nitrobenzo[1,2,5]oxadiazol-4-yl)-3-(4-nitrophenyl)urea), with some commonly investigated anions (halides, carboxylates, phosphate). In addition, two electron-withdrawing substituents, 4-nitrophenyl and nitrobenzofurazan, were appended to the 1- and 3-positions of the urea

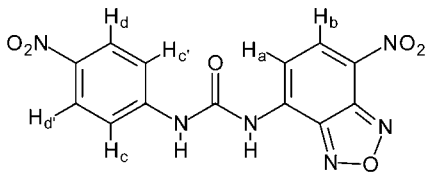

1

[a] L. Del Boca, Dr. D. Esteban-Gómez, Prof. L. Fabbrizzi, Prof. M. Licchelli, Dr. E. Monzani
Dipartimento di Chimica Generale
Università di Pavia, viale Taramelli 12
27100 Pavia (Italy)
Fax: (+39) 0382-528-544
E-mail: luigi.fabbrizzi@unipv.it

[b] Dr. M. Boiocchi
Centro Grandi Strumenti, Università di Pavia
via Bassi 21, 27100 Pavia (Italy)

 DOI: 10.1002/chem.200401049

subunit, in order to enhance both hydrogen-bond donor tendencies and acidity of the receptor. Moreover, nitrobenzofurazan is a classical chromogenic fragment,[14,15] and its colour and absorption spectrum is expected to change, following the interaction with the analyte. Noticeably, appending a chromophore (typically exhibiting electron-withdrawing properties) to the urea subunit is a normal practice for generating colorimetric anion sensors, as the occurrence of the hydrogen-bond interaction may alter the intensity of the chromophore dipole and modify its absorption spectrum.[16,17] The interaction of **1** with anions was investigated through UV-visible spectrophotometric and ^{1}H NMR spectroscopic titrations in MeCN. Such an aprotic medium was chosen in order to preclude the competition of the solvent as a hydrogen-bond donor.

Results and Discussion

The interaction with halides: On addition of F^-, the pale yellow solution of **1** (=L−H) in MeCN took an intense red colour.

Figure 1 shows the spectra recorded in the course of the titration. In particular, Figure 1 (top) displays the spectra taken during the addition of the first equivalent of fluoride: the band at 428 nm decreases and disappears, while a new band develops at 540 nm, to stop after addition of one equivalent. A definite isosbestic point at 452 nm is observed. On addition of the second equivalent of F^-, a new band develops at 382 nm, as shown in Figure 1 (bottom). We suggest that a first equilibrium is established [see Eq. (1)], leading to the formation of the hydrogen-bond complex $[L{-}H{\cdots}F]^-$, to which the band at 540 nm corresponds. Then, a second equilibrium takes place, which is tentatively represented through Equation (2), in which a further F^- ion abstracts a proton from $[L{-}H{\cdots}F]^-$, with formation of L^- and HF_2^-. In particular, the band at 382 nm should correspond to the deprotonated receptor L^-.

$$L{-}H + X^- \rightleftharpoons [L{-}H \cdots X]^- \quad (1)$$

$$[L{-}H \cdots X]^- + X^- \rightleftharpoons L^- + HX_2^- \quad (2)$$

Nonlinear least-squares treatment of spectral data gave the following values for stepwise equilibrium $\log K_1 > 6$, $\log K_2 = 4.2 \pm 0.2$. Most interestingly, on slow evaporation of a solution of **1** and excess of $[Bu_4N]F$ in MeCN, red crystals of a salt of formula $[Bu_4N]L$, suitable for X-ray diffraction studies, were obtained. The corresponding ORTEP diagram is shown in Figure 2. It is observed that a proton has been abstracted from the −NH group close to the more electron-withdrawing nitrobenzofurazan moiety.

Deprotonation induces significant structural modifications in the urea derivative **1**. In fact, previously reported structural evidence showed that 1,3-diphenyl-substituted urea molecules are completely flat, the two phenyl rings and the −HN(CO)NH− fragment lying on the same plane, in ab-

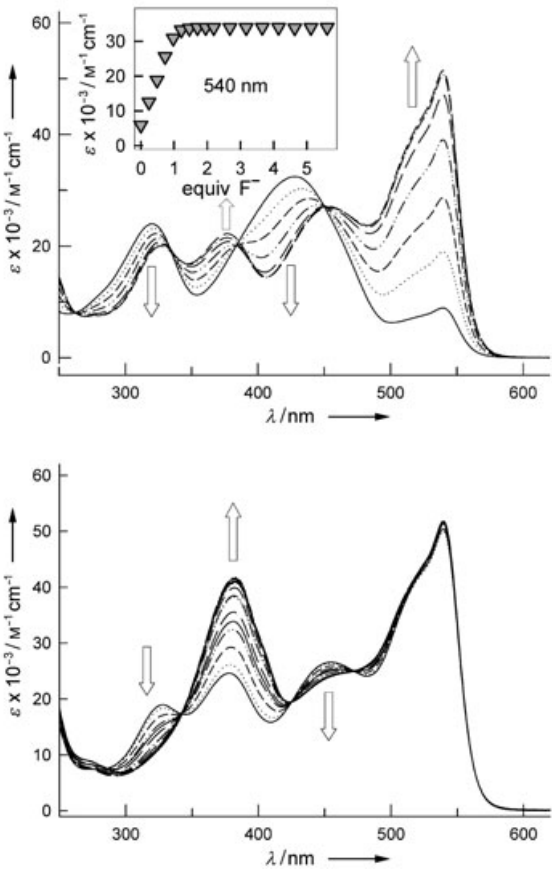

Figure 1. Family of spectra taken in the course of the titration of a solution of **1** in MeCN (4.11×10^{-5} M) with a standard solution of $[Bu_4N]F$, at 25 °C. Top: Addition of F^- up to 1.0 equiv; inset: titration profile of the band at 540 nm, which corresponds to the hydrogen-bond complex $[\mathbf{1}{\cdot}F]^-$. Bottom: Addition of F^- from 1.0 to 5.0 equiv.

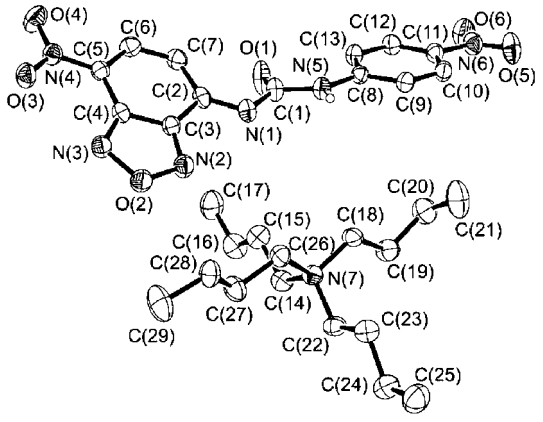

Figure 2. An ORTEP view of the $[Bu_4N]L$ salt: thermal ellipsoids are drawn at the 30% probability level, only the hydrogen atom bonded to the N(5) atom is shown. Selected bond lengths (Å) and angles (°) involving the ureate group: C(1)−O(1) 1.210(3), C(1)−N(1) 1.387(3), C(1)−N(5) 1.373(3), N(1)−C(2) 1.317(3), N(5)−C(8) 1.393(3); N(1)-C(1)-O(1) 126.7(2), N(5)-C(1)-O(1) 122.9(2), N(1)-C(1)-N(5) 110.2(2), C(1)-N(1)-C(2) 119.9(2), C(1)-N(5)-C(8) 128.7(2).

sence of steric effects between adjacent molecules.[18] On the other hand, in the L^- ion, the benzofurazan group forms a dihedral angle of 42.4(1)° with the plane containing the nitrophenyl urea subunit. Moreover, the N(1)–C(2) distance (1.317(3) Å) is significantly shorter than the N(5)–C(8) distance (1.393(3) Å), and also than that observed in other diarylureas (varying over the range 1.340–1.377 Å).[18] This suggests the occurrence of a partial delocalisation of the negative charge of the nitrogen atom towards the nitrobenzofurazan group, which is described by the resonance representation reported in Scheme 1 (structures **a** and **b**).

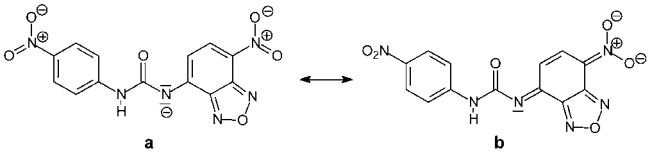

Scheme 1. A resonance representation of the deprotonated form of **1**.

In particular, on deprotonation, the phenyl ring of the furazan subunit partially loses its aromaticity, being so excluded from the extended π-system responsible for diphenylurea coplanarity. The nitrobenzofurazan fragment is then free to rotate, probably in order to minimise steric repulsions with the carbonyl oxygen atom.

Quite interestingly, each ureate ion establishes weak hydrogen-bond interactions with another close ureate ion, to give the dimer shown in Figure 3, in which each nitrobenzofurazan moiety faces the same subunit belonging to the other anion. In particular, hydrogen-bond interactions form between each –N–H fragment and the oxygen atom of the nitro group of the other ureate ion; such an atom has assumed an especially high partial negative charge due to the π-delocalisation that follows deprotonation (as emphasized by the limiting formula **b** in the resonance representation in Scheme 1).

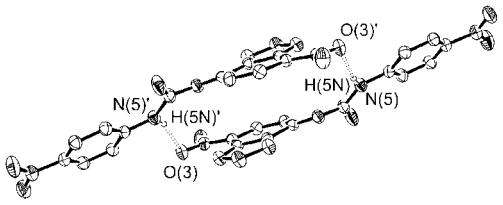

Figure 3. An ORTEP view of the ureate dimer (dashed lines show the weak N–H···O interactions and atomic labels are reported only for the atoms involved in these interactions). Features of the N–H···O interaction: N(5)–H(5N) 0.89(2) Å, H(5N)···O(3)′ 2.252(25) Å, N(5)···O(3)′ 3.111(3) Å, N(5)-H(5N)···O(3)′ 162.7(23)°, symmetry code (′) = $-x+1$, $-y$, $-z+2$.

The X-ray structural characterisation unambiguously demonstrates the fluoride-induced deprotonation of the urea fragment, and the occurrence of the stepwise equilibria given in Equations (1) and (2) has been fully corroborated by ^{1}H NMR titration experiments. Figure 4 displays the spectra recorded when a 3.00×10^{-3} M CD_3CN solution of **1** was titrated with $[Bu_4N]F$.

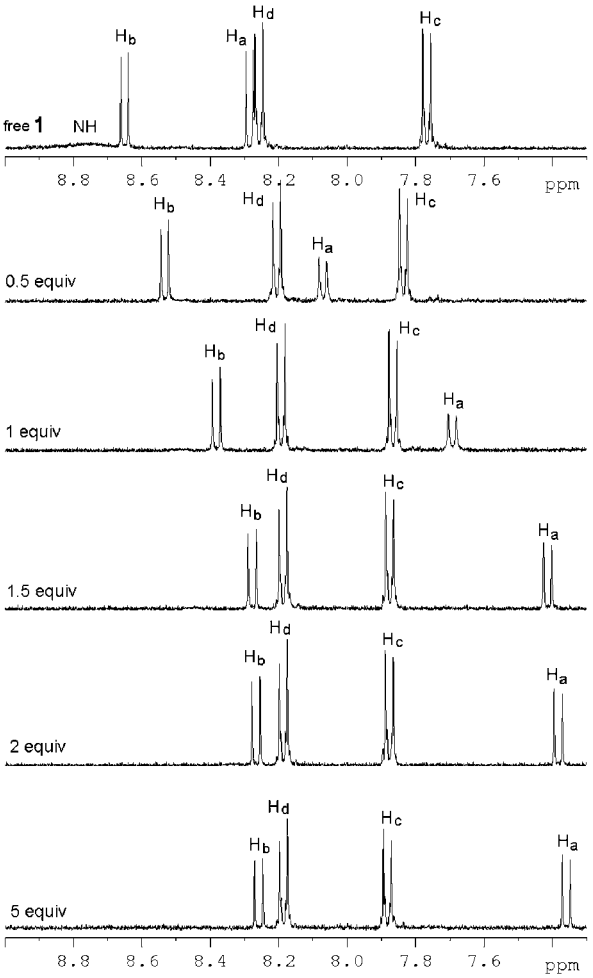

Figure 4. ^{1}H NMR spectra obtained in the course of the titration of a solution of **1** in CD_3CN (3.00×10^{-3} M) with F^-.

Two effects are expected to originate on C–H protons, following the hydrogen-bond formation between the urea subunit and the anion: 1) the increase of electron density in the phenyl rings, with a *through-bond* propagation—this causes a shielding effect and should promote an upfield shift; 2) the polarisation of the C–H bonds, induced by a *through-space* effect, electrostatic in origin—the partial positive charge created onto the proton causes a de-shielding effect and promotes a downfield shift. In fact, on addition of the first equivalent of F^-, H_a and H_b undergo upfield shift, which reflects the increase of electron density due to a through-bond effect. This supports the hypothesis that the F^- ion preferably interacts with the –NH group linked to the nitrobenzofurazan substituent. The H_c proton is, therefore, subject to a dominant electrostatic effect that induces deshielding and causes downfield shift. On the other hand, urea deprotonation, obtained on further addition of F^-, in-

duces a moderate upfield of the H_a and H_b protons (increased through-bond charge delocalisation) and has no effect on the H_c protons. In fact, the polarisation effect is no longer present, since the anion does not remain in close proximity to the receptor. It should be noted that the signals pertinent to the N–H groups of **1** are observed neither in the absence nor in the presence of fluoride. This may be ascribed to the occurrence of a fast proton exchange with water molecules that are present in solution as impurities. A similar behaviour has been observed in DMSO. Moreover, attempts were carried out to follow the formation of the $[HF_2]^-$ complex through ^{19}F NMR spectroscopy. In particular, receptor **1** was added to a Bu_4NF solution in CD_3CN. On titrant addition, the rather broad signal at −150 ppm underwent further broadening and disappearance. This may be due to the occurrence of a rather fast exchange equilibrium.

Hydrogen bonding has been defined as an incipient proton-transfer process from the hydrogen-bond donor to the acceptor.[13] The strong interaction, documented by the high value of $\log K_1$, indicates that the proton transfer has been "frozen" in a rather advanced state. Most interestingly, the addition of a second equivalent of acceptor induces a neat and definitive proton transfer, with formation of HF_2^-. This is due to the very high stability of the HF_2^- ion, which, among 1:1 hydrogen-bond complexes, shows the highest formation energy in the gas phase (39 kcal mol^{-1}).[19]

At this stage, we will try to explain the spectrophotometric behaviour observed in the course of the titration of **1** with fluoride. The nitrobenzofurazan chromophore typically presents two main absorption bands: one band centred at 300–350 nm, assigned to a π-π* transition of the aromatic group, and another band at higher wavelength, to be ascribed to the charge-transfer transition, which takes place from the linked donor group to the nitro acceptor group in the phenyl ring.[14] When the donor group is poorly donating (e.g., an amide group), the band is located between 400 and 450 nm (in MeCN). These two bands are observed in the spectrum of **1** in MeCN.

On addition of the first equivalent of fluoride, the $[\mathbf{1}\cdots F]^-$ complex forms, in which the F^- ion interacts with the N–H fragment close to the benzofurazan ring. Due to the strong hydrogen-bond interaction, the negative charge on the donor group is substantially increased, which explains the remarkable bathochromic shift to 540 nm. On addition of the second equivalent of F^-, the proton is released from the N–H group. Apparently, this does not induce any further increase of negative charge on the donor group and does not alter the intensity of the dipole: the CT band remains unmodified. On the other hand, still on addition of the second equivalent of F^-, the band at 330 nm (assigned to a π–π* transition, in the phenyl ring of the benzofurazan moiety) undergoes a bathochromic shift to 380 nm. The molecular structure of the ureate anion L^- has shown that N–H deprotonation induces drastic structural and electronic changes to the receptor. In particular, π delocalisation onto the benzofurazan moiety provokes a loss of the aromatic character of the phenyl ring, which moves towards a quinoid electronic arrangement (see the limiting formula **b** in Scheme 1). This alters the energy of π orbitals and ultimately leads to a red-shift in the optical transition. It should be noted that the spectrophotometric pattern is complicated by the presence of the nitrobenzene substituent at the other side of the urea subunit, whose optical properties may be affected, even if to a lesser extent, by complexation and deprotonation.

In a recent paper,[20] the stepwise interaction of a cyclic diamide with fluoride (anion complexation and deprotonation) was investigated through NMR studies. In particular, both complexation and deprotonation equilibria took place in the timescale of several minutes, as demonstrated by the simultaneous appearance of distinct signals for each species present at the equilibrium. Sluggishness has to be ascribed to the occurrence of conformational rearrangements of the constrained cyclic framework of the receptor. In the present study, the anion–receptor interaction was too fast, relative to the timescale of the NMR experiment, to allow the appearance of distinct signals for species at the equilibrium. This indicates the kinetically uncomplicated nature of the process.

When receptor **1** was titrated with chloride, different spectroscopic patterns were obtained. Figure 5 displays the family of UV-visible spectra recorded in the course of the titration of a 4.11×10^{-5} M solution of **1** in MeCN. Decrease of the band at 428 nm and development of the band at 540 nm were observed, as found for the previously investigated anions. However, no band development at 382 nm was detected, even after the addition of a large excess of chloride. This suggests that 1) only the equilibrium in Equation (1) takes place and 2) the hydrogen-bond complex that forms, $[L{-}H\cdots X]^-$, is stable with respect to the proton abstraction from the urea subunit. The $\log K$ value for the association equilibrium, as determined through nonlinear least-squares fitting of the smooth titration profile, is 4.05 ± 0.01.

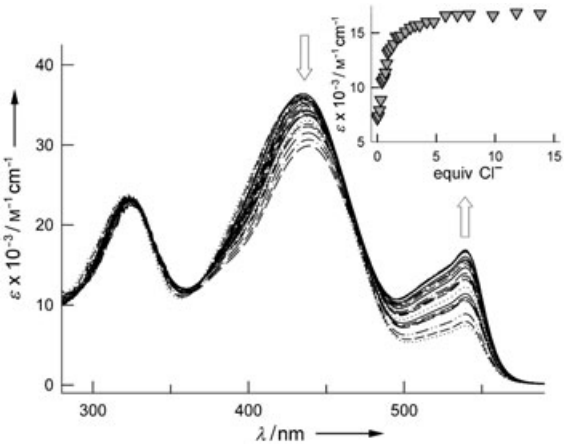

Figure 5. Family of spectra taken in the course of the titration of a solution of **1** in MeCN (4.11×10^{-5} M) with a standard solution of $[Bz(Et)_3N]Cl$, at 25 °C; inset: titration profile of the band at 540 nm, which corresponds to the hydrogen-bond complex $[\mathbf{1}\cdot Cl]^-$.

The formation of a hydrogen-bond complex of 1:1 stoichiometry has been confirmed by ^{1}H NMR titration experiments; recorded spectra are shown in Figure 6. Even on excess addition of $[BzEt_3N]Cl$, only a very moderate upfield of H_b, which reflects a weak hydrogen-bond interaction and a small through-bond effect, and a moderate downfield shift of H_c, which indicates a not too pronounced polarisation, were observed. The above behaviour has to be ascribed to the much lower basicity and hydrogen-bond acceptor properties of Cl^- with respect to F^-. In particular, Cl^- in unable to form a stable HX_2^- complex.

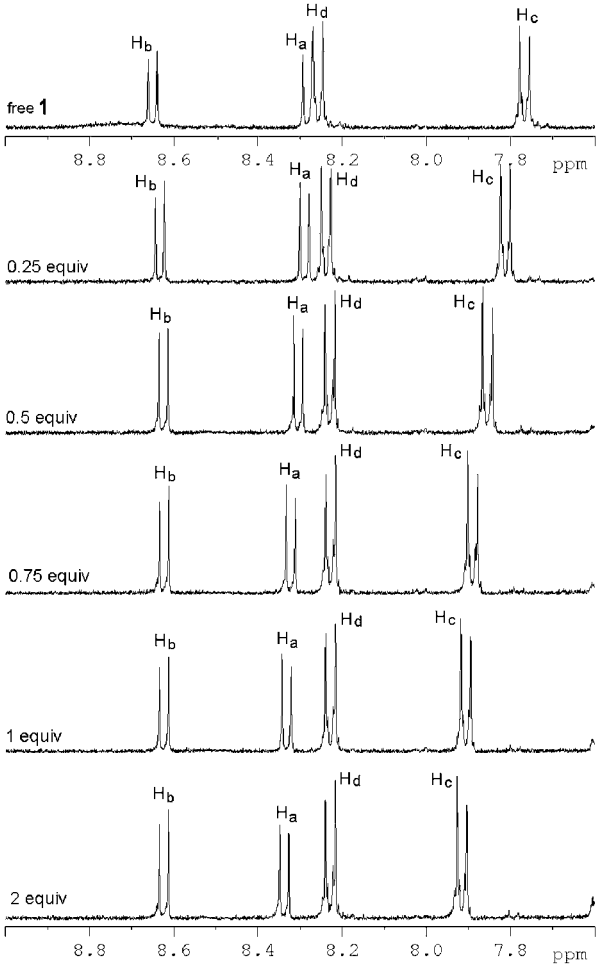

Figure 6. ^{1}H NMR spectra obtained in the course of the titration of a solution of **1** in CD_3CN (3.00×10^{-3} M) with Cl^-. Further addition of Cl^- after 1.5 equiv did not cause any further spectral change.

The interaction with oxoanions: On titration of a solution of **1** in MeCN with $[Bu_4N]CH_3COO$, $[Bu_4N]C_6H_5COO$ and $[Bu_4N]H_2PO_4$, a behaviour similar to that of fluoride was observed:

1) *UV-visible spectra*: bathochromic shift of the band at 428 nm (due to the stabilisation of the charge transfer excited state, following the formation of a 1:1 hydrogen-bond complex); development of the band at 382 nm, on addition of the second equivalent of X^-, pertinent to the deprotonated receptor.
2) *^{1}H NMR spectra*: marked upfield shift of H_a and H_b protons and downfield shift of H_c protons on addition of the first equivalent of anion; moderate upfield shift of H_a and H_b protons on further addition.

Figure 7 shows the absorption spectra taken during the titration with $[Bu_4N]CH_3COO$ of a 4.11×10^{-5} M solution of **1**. Figure 8 displays the family of ^{1}H NMR spectra obtained on titrating with acetate a 5.00×10^{-3} M solution of **1** in CD_3CN.

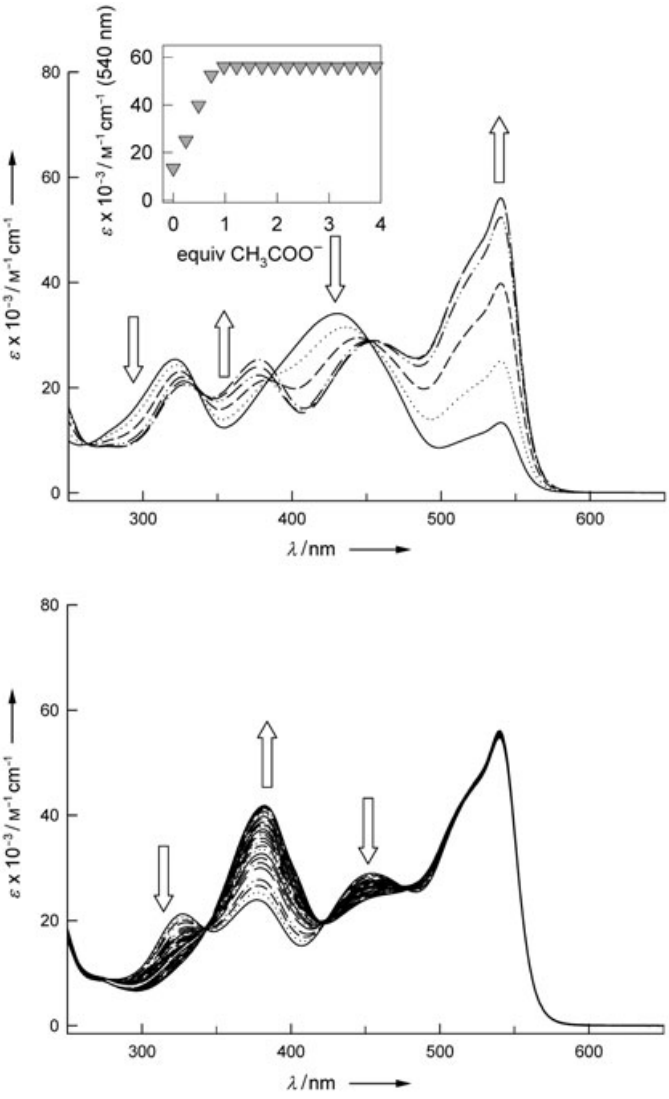

Figure 7. Family of spectra taken in the course of the titration of a solution of **1** in MeCN (4.11×10^{-5} M) with a standard solution of $[Bu_4N]CH_3COO$, at 25 °C. Top: Addition of CH_3COO^- up to 1.0 equiv; inset: titration profile of the band at 540 nm, which corresponds to the hydrogen-bond complex $[\mathbf{1}\cdot CH_3COO]^-$. Bottom: Addition of CH_3COO^- from 1.0 to 5 equiv.

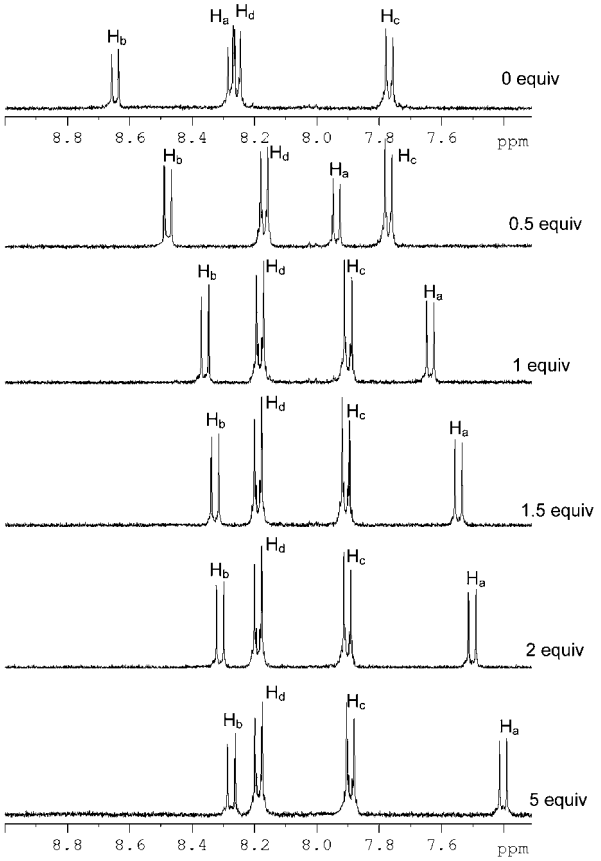

Figure 8. ^{1}H NMR spectra obtained in the course of the titration of a solution of **1** in CD_3CN (5.00×10^{-3} M) with CH_3COO^-.

The above evidence indicates that the interaction of receptor **1** with acetate, benzoate and dihydrogenphosphate proceeds according to the stepwise equilibria [Eqs. (1) and (2)], that is, formation of two directional N–H···O hydrogen bonds and deprotonation of the urea subunit, which leads to the formation of the hydrogen-bond complex involving the anion and its conjugated acid: $CH_3COO^-\cdots CH_3COOH$, $C_6H_5COO^-\cdots C_6H_5COOH$ and $H_2PO_4^-\cdots H_3PO_4$. The hypothesised geometrical arrangement of the acetic acid/acetate complex is sketched below.

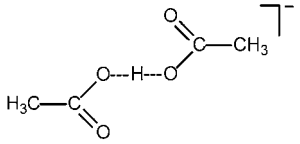

In fact, it has been stated that the most stable hydrogen-bond complexes result from the combination of fragments exhibiting similar pK_A values.[13] In particular, the most favourable case is that represented by complexes of formula $[HX_2]^-$, interfacing the X^- ion and its conjugate acid HX ($\Delta pK_A=0$), as those investigated in this work (X = F, CH_3COO, C_6H_5COO, H_2PO_4).

The constants of equilibria given in Equations (1) and (2) involving the investigated anions are reported in Table 1.

Table 1. Constants for the equilibria given in Equations (1) and (2). The standard deviation on the last figure is given in parentheses. Log$K$ values were calculated through nonlinear least-squares treatment of spectrophotometric titration data.

X^-	logK_1	logK_2
F	>6	4.2 (2)
CH_3COO^-	>6	3.8 (1)
$C_6H_5COO^-$	>6	4.0 (1)
$H_2PO_4^-$	5.40 (2)	3.83 (5)
Cl^-	4.05 (1)	–
NO_2^-	3.82 (1)	–
NO_3^-	1.99 (3)	–

On the other hand, on titration of **1** with NO_3^- and NO_2^-, patterns similar to that observed for chloride were obtained. Figure 9 shows the family of UV-visible spectra obtained on titration of **1** with $[Bu_4N]NO_2$: simultaneous disappearance of the band at 428 nm and development of a band at 540 nm were observed, with formation of a clear isosbestic point, even after addition of a large excess of anion.

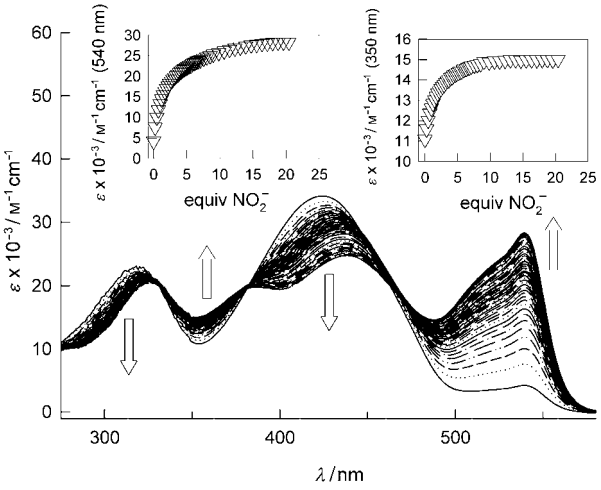

Figure 9. Family of spectra taken in the course of the titration of a solution of **1** in MeCN (4.11×10^{-5} M) with a standard solution of $[Bu_4N]NO_2$, at 25 °C; inset: titration profiles of the bands at 540 and 350 nm, which correspond to the hydrogen-bond complex $[\mathbf{1}\cdot NO_2]^-$.

This indicates the occurrence of the simple equilibrium [Eq. (1)] with formation of the hydrogen-bond complex [L–H···X]$^-$. Association constants for the NO_2^- and NO_3^- hydrogen-bond complexes are reported in Table 1.

The obtained results can be summarised as follows: all the investigated anions give a hydrogen-bond complex with receptor **1**, whose stability decreases along the series: $CH_3COO^-\approx C_6H_5O^-\approx F^->H_2PO_4^->Cl^->NO_2^->NO_3^-$ (see logK_1 values in Table 1). Such a sequence seems to parallel the hydrogen-bond acceptor tendencies of the anion. In particular, for the three oxoanions, for which the logK_1

value could be exactly determined ($H_2PO_4^-$, NO_2^-, NO_3^-), a linear relationship was found between $\log K_1$ and the average negative charge on each oxygen atom, calculated through an ab initio method: the higher the negative charge, the higher the hydrogen-bond acceptor tendencies of the anion (see Figure 10). The existence of such a relationship

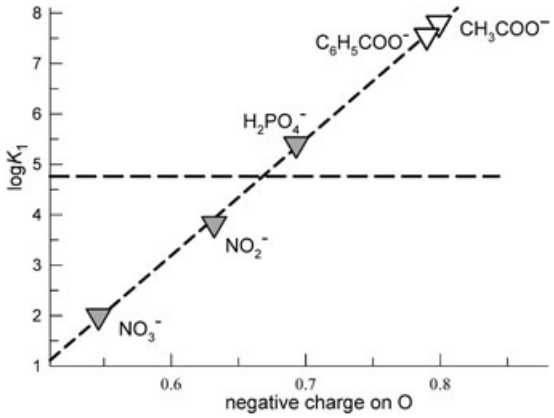

Figure 10. A linear relationship between the $\log K_1$ value for the complexation equilibrium: $\mathbf{1}+X^- \rightleftarrows [\mathbf{1}\cdot X]^-$ in MeCN and the average negative charge on the oxygen atom of the oxoanion X^- ($H_2PO_4^-$, NO_2^-, NO_3^-, gray triangles). Partial charges were calculated through an ab initio method. $\text{Log}K_1$ values for CH_3COO^- and $C_6H_5COO^-$ (white triangles) have been obtained from the least-squares straight line. The dashed horizontal line discriminates the effect of excess addition of X^-: anions above the line induce deprotonation of **1**, anions below do not and form only the hydrogen-bond complex.

indicates the purely electrostatic nature of the receptor–oxoanion interaction and leaves out any geometrical effect on the formation of the hydrogen-bond complex (e.g., matching of the distance of the N atoms of the urea subunit and the distance of the O atoms of the oxoanion). On the basis of the linear relationship, values of $\log K_1$ for acetate (7.80, from a partial charge of 0.799) and for benzoate (7.55, from a partial charge of 0.790) could be extrapolated from the least-squares straight line (see open triangles in Figure 10). Then, on addition of an excess of X^-, for the more basic anions (fluoride, carboxylates, dihydrogenphosphate), a further process takes place, which involves urea deprotonation and formation of the $[HX_2]^-$ complex. It may be surprising that proton release takes place in the most stable hydrogen-bond complexes. However, such an endoergonic term is more than compensated by the especially exoergonic term associated to the formation $[HX_2]^-$, whose stability is strictly related to the basicity of X^-. Whether addition of excess X^- induces deprotonation or not depends both on the intrinsic acidity of the urea-containing receptor and on the stability of the $[HX_2]^-$ complex. Discrimination between the two behaviours is expressed in Figure 10 by the horizontal dashed line. Anions above the line promote deprotonation and $[HX_2]^-$ formation, anions below do not. In principle, one can control the behaviour of the receptor, moving the horizontal line up and down at will, by varying the acidity of the urea subunit. Such a goal can be achieved by appending to the urea subunit substituents of different electron-withdrawing tendencies.

Conclusion

This work has elucidated the details of the urea–anion interaction: 1) on addition of the first anion equivalent, a hydrogen-bond 1:1 complex forms, the stability of which is related to the basicity of the anion (which, for oxoanions, can be expressed by the partial negative charge lying on oxygen atoms); 2) on addition of a second anion equivalent, a proton may be released by an N–H group, with formation of the $[HX_2]^-$ hydrogen-bond complex. The occurrence of the second step depends upon the intrinsic acidity of the urea subunit. Thus, when designing a urea-based receptor, one faces a paradoxical situation: the receptor's hydrogen-bond donor tendencies can be enhanced by linking electron-withdrawing groups to its framework; however, this also increases its acidity and may lead to a neutralisation process, which brings the anion out of the control of the receptor. Therefore, selectivity has to be achieved by incorporating urea fragments within a concave receptor (e.g., tripod or cage), whose shape and size match the geometrical features of the anion. However, the employed urea subunits should not be too acidic, in order to avoid –N–H deprotonation and escaping of the anion from the receptor's cavity to the solution (i.e., from the realm of supramolecular chemistry to the classic domain of Brønsted acid–base equilibria).

Experimental Section

4-Amino-7-nitro-2,1,3-benzoxadiazole: 4-Chloro-7-nitro-2,1,3-benzoxadiazole (0.023 g, 0.1632 mmol) was disolved in methanol (10 mL). After the addition of ammonia (0.7 mL), the mixture was stirred for 12 h. The reaction mixture was evaporated to dryness under reduced pressure and the residue was subjected to chromatography on silica gel with AcOEt/hexane (3:2) to afford (0.111 g, 62%) an air-stable brown powder. ^{1}H NMR ($CDCl_3$): $\delta = 8.46$ (d, $J = 8.0$ Hz, 1H), 6.41 ppm (d, $J = 8.0$ Hz, 1H); ESI-MS: m/z: 181 $[M+H]^+$.

1-(7-Nitrobenzo[1,2,5]oxadiazol-4-yl)-3-(4-nitrophenyl)urea (1): 4-Nitrophenylisocyanate (0.027 g, 0.1638 mmol) was added into an argon-filled reactor containing 4-amino-7-nitro-2,1,3-benzoxadiazole (0.030 g, 0.164 mmol) in dry dioxane (10 mL). The mixture was heated at 60 °C under magnetic stirring for 1 h and then left under magnetic stirring for 12 h. During the reaction, a light orange precipitate appeared, which was collected by filtration, washed with water and dried under vacuum. The product (0.020 g, 36%) is air-stable in the solid state and soluble in all common organic solvents. ^{1}H NMR (CD_3CN): $\delta = 8.78$ (br, 2H; NH), 8.65 (d, $J = 8.0$ Hz, 1H; H_b), 8.29 (d, $J = 8.0$ Hz, 2H; H_a), 8.25 (d, $J = 8.1$ Hz, 2H; H_d), 7.77 ppm (d, $J = 8.1$ Hz, 2H; H_c); IR (nujol mull): $\tilde{\nu} =$ 1736 (C=O), 1558 ($\nu_{as}(NO_2)$), 1310, 1282 ($\nu_s(NO_2)$), 3382, 3325 (ν_{as},ν_s(N–H)), 1446, 1202 (δ_{as},δ_s(N–H)).

General procedures and materials: All reagents were purchased by Aldrich/Fluka and used without further purification. UV/Vis spectra were recorded on a Varian CARY 100 spectrophotometer, with a quartz cuvette (path length: 1 cm). NMR spectra were recorded on a Bruker Avance 400 spectrometer, operating at 9.37 T. Spectrophotometric titrations were performed at 25 °C on 10^{-4} and 10^{-5} M solutions of **1** in MeCN.

Typically, aliquots of freshly prepared Bu_4NX standard solutions were added and the UV/Vis spectra of the samples were recorded. All spectrophotometric titration curves were fitted with the HYPERQUAD program.[21] ^1H NMR titrations were carried out in CD_3CN.

X-ray crystallographic studies: Single crystals of $[Bu_4N]L$, suitable for X-ray crystallography, were grown by slow diffusion of diethyl ether into a solution of **1** in THF in the presence of excess $[Bu_4N]F$. Crystal data for $[Bu_4N]L$ salt: $C_{29}H_{43}N_7O_6$, $M_r = 585.70$, $T = 293$ K, crystal dimensions $0.55 \times 0.10 \times 0.10$ mm^3, monoclinic, $P2_1/n$ (No. 14), $a = 9.8165(6)$, $b = 16.1456(10)$, $c = 20.2528(13)$ Å, $\beta = 102.466(2)$, $V = 3134.3(3)$ Å^3, $Z = 4$, $\rho_{calcd} = 1.241$ g cm^{-3}, $F(000) = 1256$, $\mu = 0.088$ mm^{-1}, $Mo_{K\alpha}$ X-radiation ($\lambda = 0.7107$ Å), $2\theta_{max} = 60°$, 27066 measured reflections, 9173 independent reflections ($R_{int} = 0.061$), 3765 strong reflections [$I_o > 2\sigma(I_o)$], 386 refined parameters, $R1 = 0.0658$ (strong data) and 0.1720 (all data), $wR2 = 0.1496$ (strong data) and 0.2007 (all data), GOF = 0.966, 0.25/−0.24 max/min residual electron density. Diffraction data were collected at ambient temperature on a Bruker-Axs Smart-Apex CCD-based diffractometer. Omega rotation frames (scan width 0.3°, scan time 30 s, sample-to-detector distance 5 cm) were processed with the SAINT software (Bruker-Axs) and intensities were corrected for Lorentz and polarisation effects. Absorption effects were analytically evaluated by the SADABS software,[22] and correction was applied to the data (0.96/0.99 min/max transmission factor). The structure was solved by direct methods (SIR-97),[23] and refined by full-matrix least-square procedures on F^2 using all reflections (SHELXL-97).[24] Calculations were performed with the WinGX package.[25] All non-hydrogen atoms were refined with anisotropic temperature factors. Hydrogen atoms bonded to carbon atoms were placed by using the appropriate AFIX instructions, the hydrogen atom bonded to the N(5) amine was located in the ΔF map and refined without constraint on the atomic coordinate. CCDC 244867 contains the supplementary crystallographic data for this paper. These data can be obtained free of charge from The Cambridge Crystallographic Data Centre via www.ccdc.cam.ac.uk/data_request/cif.

Acknowledgements

The financial support of the European Union (RTN Contract HPRN-CT-2000-00029) and of the Italian Ministry of University and Research (PRIN—Dispositivi Supramolecolari; FIRB—Project RBNE019H9K) is gratefully acknowledged.

[1] P. A. Gale, *Coord. Chem. Rev.* **2003**, *240*, 1–226.
[2] P. D. Beer, P. A. Gale, Angew. Chem. **2001**, *99*, 502–532; *Angew. Chem. Int. Ed.* **2001**, *40*, 486–516.
[3] F. P. Schmidtchen, M. Berger, *Chem. Rev.* **1997**, *97*, 1609–1646.
[4] P. J Smith, M. V. Reddington, C. S. Wilcox, *Tetrahedron Lett.* **1992**, *33*, 6085–6088.
[5] E. Fan, S. A. van Arman, S. Kincaid, A. D. Hamilton, *J. Am. Chem. Soc.* **1993**, *115*, 369–370.
[6] J. Scheerder, J. F. J. Engbersen, A. Casnati, R. Ungaro, D. N. Reinhoudt, *J. Org. Chem.* **1995**, *60*, 6448–6454.
[7] M. P. Hughes, M. Shang, B. D. Smith, *J. Org. Chem.* **1996**, *61*, 4510–4511.
[8] M. P. Hughes, B. D. Smith, *J. Org. Chem.* **1997**, *62*, 4492–4499.
[9] R. J. Fitzmaurice, G. M. Kyne, D. Douheret and J. D. Kilburn, *J. Chem. Soc. Perkin Trans. 1* **2002**, 841–864.
[10] A. J. Evans, S. E. Matthews, A. R. Cowley, P. D. Beer, *Dalton Trans.* **2003**, 4644–4650.
[11] H. Miyaji, S. R. Collinson, I. Prokes, J. H. R. Tucker, *Chem. Commun.* **2003**, 64–65.
[12] M. Barboiu, G. Vaughan, A. van der Lee, *Org. Lett.* **2003**, *5*, 3074–3076.
[13] T. Steiner, *Angew. Chem.* **2002**, *114*, 50–80; *Angew. Chem. Int. Ed.* **2002**, *41*, 48–76.
[14] S. Uchiyama, T. Santa, K. Imai, *J. Chem. Soc. Perkin Trans. 2* **1999**, 2525.
[15] B. Ramachandram, A. Samanta, *J. Phys. Chem. A* **1998**, *102*, 10579–10587.
[16] C. Suksai, T. Tuntulani, *Chem. Soc. Rev.* **2003**, *32*, 192–202.
[17] R. Martínez-Mañez, F. Sancenón, *Chem. Rev.* **2003**, *103*, 4419–4476.
[18] M. C. Etter, Z. Urbanczyk-Lipkowska, M. Zia-Ebrahimi, T. W. Panunto, *J. Am. Chem. Soc.* **1990**, *112*, 8415–8426.
[19] S. Gronert, *J. Am. Chem. Soc.* **1993**, *115*, 10258–10266.
[20] A. M. Costero, M. J. Bañuls, M. J. Aurell, M. D. Ward, S. Argent, *Tetrahedron* **2004**, *60*, 9471–9478.
[21] P. Gans, A. Sabatini, A. Vacca, *Talanta* **1996**, *43*, 1739–1753.
[22] G. M. Sheldrick, SADABS, Siemens Area Detector Absorption Correction Program, University of Göttingen (Germany), **1996**.
[23] A. Altomare, M. C. Burla, M. Cavalli, G. L. Cascarano, C. Giacovazzo, A. Guagliardi, A. G. G. Moliterni, G. Polidori, R. Spagna, *J. Appl. Crystallogr.* **1999**, *32*, 115–119.
[24] G. M. Sheldrick, SHELX-97, Programs for Crystal Structure Analysis, University of Göttingen (Germany), **1997**.
[25] L. J. Farrugia, *J. Appl. Crystallogr.* **1999**, *32*, 837–838.

Received: October 14, 2004
Published online: March 15, 2005